Targeted Drug Delivery

International Edition: DOI: 10.1002/anie.201500183
German Edition: DOI: 10.1002/ange.201500183

Photochemical Internalization of Tamoxifens Transported by a "Trojan-Horse" Nanoconjugate into Breast-Cancer Cell Lines**

Theodossis A. Theodossiou, A. Ricardo Gonçalves, Konstantina Yannakopoulou, Ellen Skarpen, and Kristian Berg*

Abstract: *Photochemical internalization (PCI) has shown great promise as a therapeutic alternative for targeted drug delivery by light-harnessed activation. However, it has only been applicable to therapeutic macromolecules or medium-sized molecules. Herein we describe the use of an amphiphilic, water-soluble porphyrin–β-cyclodextrin conjugate (mTHPP-βCD) as a "Trojan horse" to facilitate the endocytosis of CD-guest tamoxifens into breast-cancer cells. Upon irradiation, the porphyrin core of mTHPP-βCD expedited endosomal membrane rupture and tamoxifen release into the cytosol, as documented by confocal microscopy. The sustained complexation of mTHPP-βCD with tamoxifen was corroborated by 2D NMR spectroscopy and FRET studies. Following the application of PCI protocols with 4-hydroxytamoxifen (4-OHT), estrogen-receptor β-positive (Erβ+, but not ERβ−) cell groups exhibited extensive cytotoxicity and/or growth suspension even at 72 h after irradiation.*

Photodynamic therapy of cancer (PDT)[1] is a treatment modality which utilizes a photosensitive drug (photosensitizer, PS), light of the appropriate wavelength, and molecular oxygen as the terminal acceptor of energy or electrons to form singlet oxygen or other deleterious reactive oxygen species (ROS). These species cause local irreversible photodamage to biological substrates within the region of irradiation. A promising evolution of PDT came through the concept of photochemical internalization (PCI).[2] PCI is actually a light-controlled drug- and gene-delivery modality[3] in which light activation enables spatiotemporal specificity and control over the intracellular drug release. The principle of PCI lies in drug endocytosis. Cells are treated with an amphiphilic PS with high affinity for the plasma membrane (e.g. Amphinex), so that the PS subsequently remains in the membranes of the endosomal vesicles following endocytosis. The cells are simultaneously treated with drugs or molecules that cannot passively enter cells owing to their unfavorable properties (e.g. hydrophilicity, large size, or negative charge). The drugs are endocytosed and thus confined in endosomes and lysosomes with photosensitizers anchored on their membranes. Upon selective irradiation with light of the appropriate wavelength, the formed ROS, and especially $^1O_2$, may cause lipid peroxidation[4] to the endosomal membranes. This transformation potentiates membrane rupture with concomitant release of the endosomal load, thus leading to the cytoplasmic release of a drug at high concentrations specifically in irradiated tissues.

Until now, PCI has been developed and documented for the delivery of therapeutic biomacromolecules and medium-sized molecules, which are unable to enter cells in any other manner than endocytosis. However, the majority of the most efficient, widely used, and approved cancer therapeutics are small molecules, which can freely enter both target and nontarget cells by passive diffusion. The use of PCI technology for the specific delivery of such molecules to cancer lesions in doses much higher than those used in chemotherapy would minimize side effects to normal tissues. There are numerous other techniques based on small-molecule caging with photocleavable cages or containers;[5] however, PCI is unique in its use of the endocytic vesicles as photolabile confinement compartments for the drugs to be delivered.

The synthesis of nanosized molecular carriers that are capable of transporting and releasing chemotoxic agents into a biological target, preferably in a controlled manner, is an important objective of contemporary drug-delivery research. The ideal carrier would combine different functionalities, sufficient water solubility, and the capacity to be internalized by cells in vitro and in vivo. Cyclodextrins (CDs), water-soluble macrocyclic oligosaccharides and approved drug excipients, are commonly used to facilitate drug dissolution in aqueous solutions though inclusion-complex formation as the major mechanism. The covalent attachment of a CD moiety to a PS has been envisaged as a strategy to combine the drug-encapsulation and solubilization capacity of the CD moiety with the photosensitizing/fluorescence-imaging properties of the PS moiety, especially in the case of nonionic porphyrins, which are notorious for their lack of aqueous solubility. 5,10,15,20-Tetrakis(*m*-hydroxyphenyl)-21,23*H*-por-

[*] Dr. T. A. Theodossiou, Dr. E. Skarpen, Prof. K. Berg
Department of Radiation Biology (T.A.T., K.B.) and Department of Biochemistry (E.S.), Institute for Cancer Research
The Norwegian Radium Hospital, Oslo University Hospital
Montebello, 0379 Oslo (Norway)
E-mail: Theodossis.Theodossiou@rr-research.no
A. R. Gonçalves, Dr. K. Yannakopoulou
Institute of Nanoscience and Nanotechnology
NCSR "Demokritos", Patriarchou Gregoriou and Neapoleos
Ag. Paraskevi, Attiki, 15310 (Greece)

[**] K.B. and T.A.T. gratefully acknowledge the European Community for financially supporting this research through the Marie Curie Intra-European Fellowship HYPERTAM (327075). K.Y. and A.R.G. thank the Marie Curie Program No. 237962 CYCLON (FP7-PEOPLE-ITN-2008) for financial support to MC fellow A.R.G. and funding of the research. Moreover, A.R.G. is indebted to Assoc. Prof. Helena Cabral-Marques, Faculty of Pharmacy, University of Lisbon, for helpful discussions and support. Finally, we thank Seahorse Biosciences for the kind loan of a Seahorse XFe96 Analyzer, which made the metabolic studies possible.

Supporting information for this article is available on the WWW under http://dx.doi.org/10.1002/anie.201500183.

phyrin (mTHPP, Scheme 1a) is a nonionic, water-insoluble PS, the porphyrin analogue of the clinically used chlorin temoporfin (marketed as Foscan). We recently reported[6] the efficient synthesis and molecular characterization of

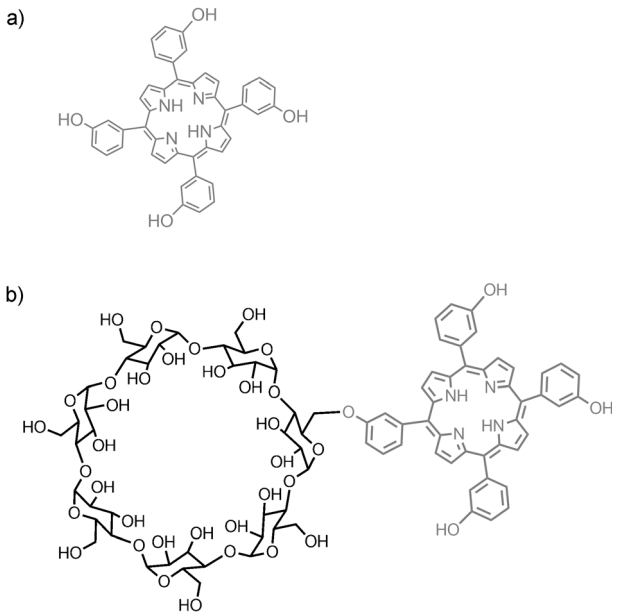

Scheme 1. Chemical structures of a) mTHPP and b) mTHPP-βCD.

a mTHPP-βCD conjugate (Scheme 1b), which displayed improved emission properties in aqueous media as compared to those of mTHPP alone and aqueous solubility in the biologically relevant micromolar range. Moreover, mTHPP-βCD proved to be a photoresponsive multifunctional nanocarrier with the combined capacity to release ROS and transport a nitric oxide releasing guest.[6]

In the current study, we investigated the PCI potential of the mTHPP-βCD conjugate with tamoxifens as guest molecules. Tamoxifen (TAM) is a nonsteroidal selective estrogen-receptor modulator (SERM) applicable to the treatment of estrogen-responsive cancers, such as breast cancer.[7] *N*-Desmethyltamoxifen (NDMTAM) and *trans*-4-hydroxytamoxifen (4-OHT), the major metabolites of tamoxifen, exhibit estrogen-receptor affinities comparable to that of 17β-estradiol.[8] TAM binds to cell estrogen receptors (ERs) stimulating cytostasis[7b] or cell-apoptosis propagation.[9] TAM-induced cell death has, however, been observed both in estrogen-receptor-positive and estrogen-receptor-negative cell lines,[10] thus suggesting a nongenomic component of TAM action. In a previous study,[11] we demonstrated that fluorescein isothiocyanate (FITC)-conjugated NDMTAM localized in cell mitochondria and the endoplasmic reticulum.

To document the formation of inclusion complexes between mTHPP-βCD and NDMTAM by NMR spectroscopy, a gigantic leap in the aqueous solubility of mTHPP-βCD was required, from micromolar to millimolar concentrations. This solubility improvement was accomplished by the use of heptakis(2,3,6-*O*-methyl)-β-cyclodextrin (pMβCD, in which the "p" stands for "per") as an effective yet noninterfering solubilizer. pMβCD has been shown to form very strong inclusion complexes with porphyrins in aqueous environments.[12] In good agreement with the previously reported studies, strong diastereoisomeric 1:1 inclusion complexes between mTHPP-βCD and pMβCD were formed with $K_{11} = 3.8(\pm 1.6) \times 10^6\,\text{M}^{-1}$ ($R^2 = 0.9954$), thus resulting in a solubility of approximately 2 mM. NMR spectra unequivocally showed that the βCD cavity of mTHPP-βCD remained available for further complex formation, as the pMβCD unit was found to be stationed exclusively on the mTHPP moiety (Figure 1; see

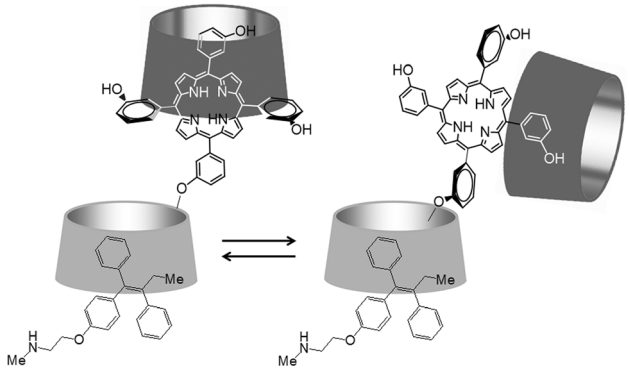

Figure 1. Solution structure of mTHPP-βCD/pMβCD/NDMTAM as a 1:1 mixture of diastereoisomeric complexes, as derived from NMR spectroscopic data. βCD: light gray; pMβCD: dark gray.

also the Supporting Information, including Figures S1–S5). Moreover, the mTHPP-βCD/pMβCD nanosystem in 4% dimethyl sulfoxide (DMSO) either in phosphate-buffered saline solution (PBS) or in D_2O was shown to encapsulate NDMTAM via either one of its unsubstituted phenyl groups, and the drug solubility increased by a factor of four, thus demonstrating the capability of the conjugate, even in complex with pMβCD, to solubilize the drug by inclusion (see Figure S6).

Förster resonance energy transfer (FRET) studies were performed between mTHPP-βCD and NDMTAM covalently attached to FITC (NDMTAM-FITC). The FRET wavelength was set to 488 nm, which is optimal for FITC but not for the porphyrin moiety (minimal absorbance). The strong FRET observed from NDMTAM-FITC to mTHPP-βCD (Figure 2) indicated that the NDMTAM-FITC moiety remained encapsulated, in good agreement with 2D NOESY spectra (see Figure S6), and further showed that the complexation is not abolished in serum-containing media.

Representative confocal images of MCF7 estrogen-receptor β-positive (Erβ+) and MDA-MB-231 (Erβ−) breast human carcinoma cells loaded with mTHPP-βCD/NDMTAM-FITC, pre- and postirradiation, are shown in Figure 3. The quenching of FITC fluorescence before irradiation can be attributed either to FRET from the FITC to the mTHPP moiety owing to their close proximity (as in solution, Figure 2) or to π–π interactions and the formation of aggregates that favor energy dissipation through nonirradiative processes. FITC fluorescence is also known to be attenuated at the pH value of lysosomes. The red mTHPP-βCD fluorescence is punctate (Figure 3, middle column), in

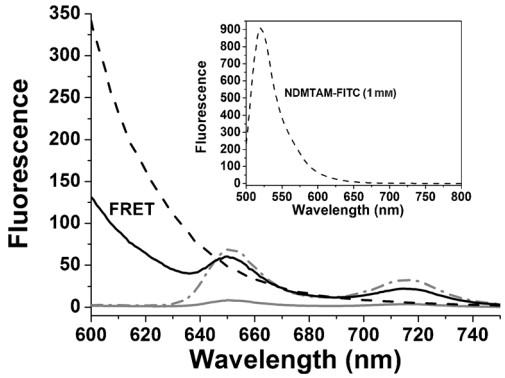

Figure 2. FRET spectra between mTHPP-βCD and NDMTAM-FITC in RPMI 1640 medium containing 10% fetal calf serum. NDMTAM-FITC (7.5 μM) fluorescence occurs at $\lambda_{ex}=488$ nm (black dashed line). mTHPP-βCD fluorescence is shown as a gray line with a dash–dot pattern (registered following excitation at 410 nm of a 10 μM mTHPP-βCD solution). The same solution upon excitation at 488 nm yielded the spectrum depicted with a solid gray line. Fluorescence of the mTHPP-βCD (10 μM)/NDMTAM-FITC (7.5 μM) complex is shown as a solid black trace ($\lambda_{ex}=488$ nm, FRET). Inset: Fluorescence of 1 μM NDMTAM-FITC ($\lambda_{ex}=488$ nm).

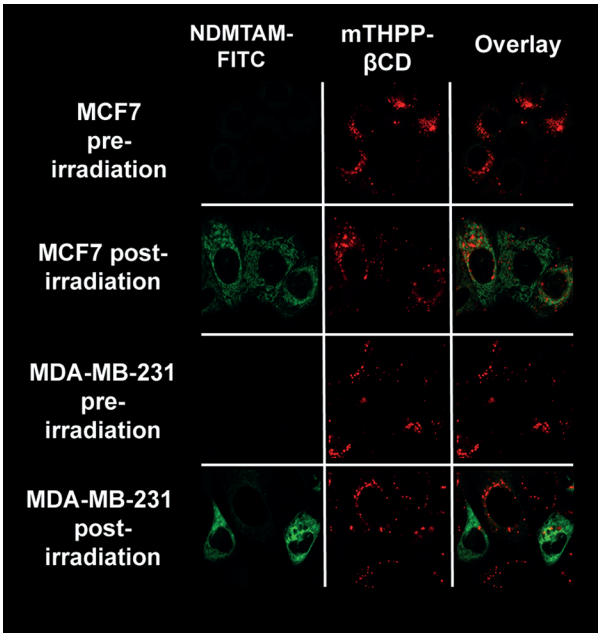

Figure 3. Confocal microscopy images of MCF7 and MDA-MB-231 cells treated with mTHPP-βCD/NDMTAM-FITC overnight (16 h). MCF7 cells were irradiated with a 2 J cm^{-2} dose and MDA-MB-231 cells with a 1.4 J cm^{-2} dose of red light, and images were acquired approximately 4 min later (see Figure S9). The micrographs of cells prior to and after light exposure are not from the same area of the dish.

agreement with subcellular accumulation in endocytic vesicles, as also shown by our colocalization studies with dextran-FITC (see Figure S12). Upon irradiation, monomeric photosensitizer, relocated quite possibly in close proximity to the endosomal membranes, is activated and rupture the endosomal membranes according to the PCI principle.[2] Upon endosomal-membrane compromise, the endocytosed species are liberated into the cell cytosol. In both cell lines, it was NDMTAM-FITC fluorescence that increased after irradiation (Figure 3). This result is attributed to dislocation of the NDMTAM-FITC molecules from the mTHPP-βCD cavities. The dislodged NDMTAM-FITC molecules are redistributed perinuclearly, most likely to mitochondria and/or the endoplasmic reticulum, which have been previously shown to be the subcellular accumulation loci for NDMTAM-FITC.[11] On the other hand, mTHPP-βCD fluorescence did not exhibit any radical relocalization following irradiation. The PCI-induced translocation of drugs and the photosensitizer itself into the cytosol has been found to take some time and may take as long as 1 h.[13] The singlet oxygen formed has a very short lifetime (submicrosecond level) but induces lipid-peroxidation chain reactions that may last for approximately 20–40 min.[14] Thus, the present results are consistent with the photochemically induced release of tamoxifen from mTHPP-βCD within the endocytic vesicles.

Unbound tamoxifen can freely pass cellular membranes, and this process is rapid (Figure 3). Initially, the photocytotoxicity light-dose response curves (PDT effect) were determined for cells treated with mTHPP-βCD (10 μM) overnight (see Figure S7). From these curves, the LD_{50} values were extracted for both cell lines (4 J cm^{-2} for MCF7 cells, 2.7 J cm^{-2} for MDA-MB-231 cells). The PCI effect of the complex mTHPP-βCD(10 μM)–4-OHT(7.5 μM) was subsequently assessed in the two cell lines. We used four treatment groups: incubation with the vehicle (medium controls), 4-OHT (7.5 μM), mTHPP-βCD (10 μM; PDT group), and mTHPP-βCD(10 μM)–4-OHT(7.5 μM) (PCI group) for 16 h. All cell groups (except dark controls) were irradiated at their LD_{50} light-dose values. We subjected the cells to standard MTT assays at 24, 48, and 72 h postirradiation to determine their viability. The toxicity data for the control experiments in the dark for all the above groups show (see Figure S8) that all compounds have limited chemical toxicity: In MCF7 cells the maximal toxicity in the dark was seen for incubation with the complex mTHPP-βCD(10 μM)–4-OHT(7.5 μM) ($\leq 40\%$), whereas for MDA-MB-231 the equivalent value was about 20%. Accordingly, the corresponding chemical toxicities for incubation with mTHPP-βCD were found to be about 20 and 10%, respectively.

The phototoxicities for the four treatment groups are shown in Figure 4. The two cell lines behaved quite differently. In the MCF7 PDT cell group, profound phototoxicity was observed at 24 h postirradiation (ca. 70%). This phototoxicity, however, was gradually abrogated at 48 and 72 h, presumably owing to the proliferation of surviving cells. In the PCI group, cell death was much more profound (ca. 80%) and remained unchanged at both the 48 and 72 h assay time points. This result implies a profound PCI effect in Erβ+ cells, which are genomically affected by the SERM 4-OHT. In this sense, PCI presumably suppressed the abrogation of the PDT effect by the release in the cell cytosol of substantial amounts of 4-OHT, which engaged the available subcellular SERM targets. The fact that 4-OHT alone conferred no substantial toxicity to MCF7 cells in the absence or presence of light shows that the regime of administration (7.5 μM, 16 h) was sublethal to the cells and the sustained toxicity conferred to

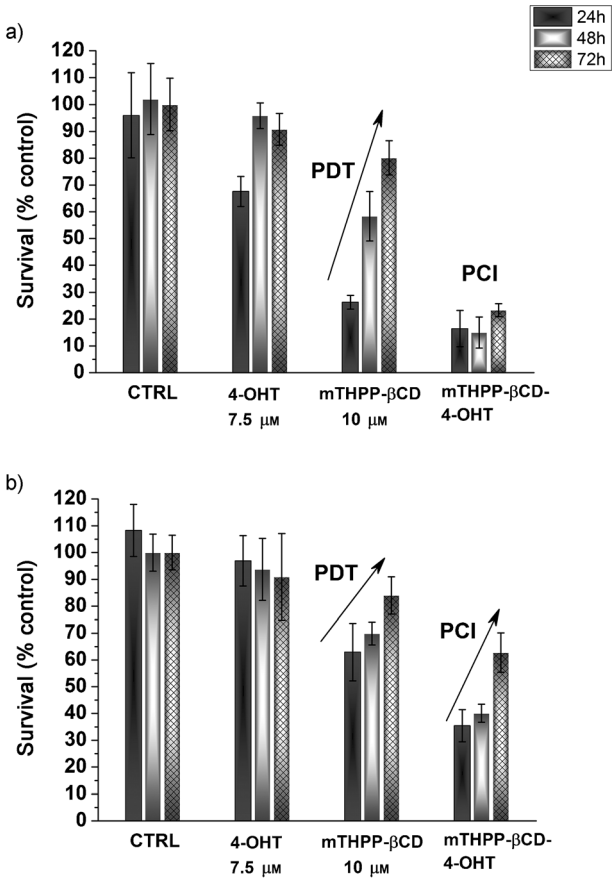

Figure 4. Photocytotoxicity to A) MCF7 and B) MDA-MB-231 cells following overnight (16 h) incubation with medium only (CTRL), 4-OHT (7.5 μM), mTHPP-βCD (10 μM), and mTHPP-βCD(10 μM)–4-OHT(7.5 μM). All groups were irradiated at the LD_{50} light doses (see the Supporting Information). The MTT assays were performed at 24, 48, and 72 h postirradiation.

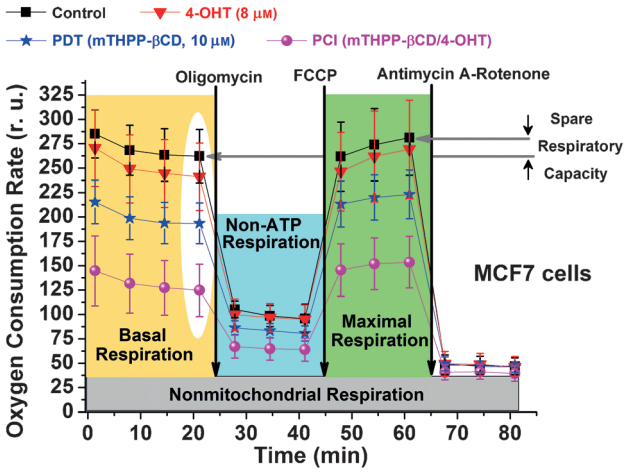

Figure 5. Changes induced by mTHPP-βCD PDT and mTHPP-βCD–4-OHT PCI in the respiration of MCF7 cells. Cell respiration was monitored by measurement of the oxygen-consumption rate (OCR) with a Seahorse XFe96 Analyzer. The equilibrated basal respiration values of interest are highlighted in white, and the response to mitochondrial stress induced by various electron-transport-chain (ETC) inhibitors is shown for all cell groups.

the PCI group is solely attributable to the large amounts of 4-OHT released intracellularly upon cell irradiation. In the case of MDA-MB-231 cells, the nongenomic photochemically induced chemotoxicity was less profound, but it was also gradually abrogated (lower at 72 h). Further clonogenic survival studies (see Figure S13) confirmed that the PCI effects shown in Figure 4 are not cytostatic, but clearly cytotoxic, since only about 5 % of the PCI-treated MCF7 cells retained the ability to form clones. In the case of MDA-MB-231 cells, PCI did not add significantly to the PDT cytotoxicity.

The main advantage of using the mTHPP-βCD conjugate as a host for 4-OHT is the fact that PCI up to now has only been applicable to a large variety of macromolecules (>1000 Da) that do not readily transverse the plasma membrane, including immunotoxins based on type I ribosome-inactivating protein toxins, poly- and oligonucleotide therapeutics, and chemotherapeutic agents, such as bleomycin (1400 Da).[15] PCI has until now not been applicable to small molecules, such as 4-OHT, which instead of being endocytosed, freely penetrate the cell membranes owing to their physicochemical properties (e.g. small size, hydrophobicity, positive charge).

We also performed metabolic studies with a Seahorse XFe96 Analyzer. The profound effects of mTHPP-βCD–4-OHT PCI on MCF7 respiratory capacity are shown in Figure 5. The basal respiration, as reflected by the oxygen-consumption rate (OCR), underwent a very profound decrease following PCI treatment. The effect was even greater than that in the PDT (mTHPP-βCD-vehicle-treated) group. In contrast, the glycolytic rate remained comparable between the treatment groups (see Figure S10). The above metabolic changes were observed 1 h after irradiation of the PDT and PCI groups; no significant respiratory (OCR) changes between the control, tamoxifen (4-OHT), PDT (mTHPP-βCD + light), and PCI (mTHPP-βCD–4-OHT + light) were observed in the case of MDA-MB-231 cells, which exhibited an approximately fivefold lower basal respiration than that of MCF7 cells (see Figure S11 A). The MCF7 respiratory changes are attributed to the large 4-OHT payload released intracellularly by PCI, whereas in the case of incubation with free 4-OHT, the internalized amount was limited by equilibrium dynamics. The corresponding metabolic studies for MDA-MB-231 cells (see Figure S11) showed no significant discrepancies between treatment groups and thus confirmed the differential effect of the controlled release of the 4-OHT payload within MCF7 cells. In all metabolic studies, the inhibitors helped establish that the respiration was not uncoupled from ATP production and that the respiration was not completely inhibited.

In the present study, the mTHPP-βCD conjugate functioned like a "Trojan horse" to keep the complexed tamoxifen moieties "hidden" so that they would be endocytosed together with the carrier macromolecule conjugate and remain confined until the complex was released from the endocytic vesicles upon irradiation. PCI has the unique advantage of controlled drug delivery and release upon activation with light. Also, drugs can be released specifically

in the irradiated areas of cells at much larger concentrations than those attainable by systemic administration owing to the need to avoid (or limit) unwanted side effects to the patient. The present study establishes the applicability of PCI technology to a huge variety of small molecules with well-documented and clinically approved anticancer activities whose use was hitherto restricted by the lack of a means of specific delivery to cancerous lesions.

Keywords: antitumor agents · cyclodextrins · drug delivery · photochemical internalization · porphyrinoids

How to cite: *Angew. Chem. Int. Ed.* **2015**, *54*, 4885–4889
Angew. Chem. **2015**, *127*, 4967–4971

[1] a) A. J. Macrobert, T. Theodossiou in *Encyclopedia of Modern Optics*, *Vol. 1* (Ed.: R. D. Guenther), Elsevier, Amsterdam, **2005**, pp. 53–62; b) P. Agostinis, K. Berg, K. A. Cengel, T. H. Foster, A. W. Girotti, S. O. Gollnick, S. M. Hahn, M. R. Hamblin, A. Juzeniene, D. Kessel, M. Korbelik, J. Moan, P. Mroz, D. Nowis, J. Piette, B. C. Wilson, J. Golab, *CA: A Cancer Journal for Clinicians* **2011**, *61*, 250–281.

[2] K. Berg, P. K. Selbo, L. Prasmickaite, T. E. Tjelle, K. Sandvig, J. Moan, G. Gaudernack, Ø. Fodstad, S. Kjølsrud, H. Anholt, G. H. Rodal, S. K. Rodal, A. Høgset, *Cancer Res.* **1999**, *59*, 1180–1183.

[3] a) K. Berg, M. Folini, L. Prasmickaite, P. K. Selbo, A. Bonsted, B. O. Engesaeter, N. Zaffaroni, A. Weyergang, A. Dietze, G. M. Maelandsmo, E. Wagner, O.-J. Norum, A. Hogset, *Curr. Pharm. Biotechnol.* **2007**, *8*, 362–372; b) A. Høgset, L. Prasmickaite, P. K. Selbo, M. Hellum, B. Ø. Engesaeter, A. Bonsted, K. Berg, *Adv. Drug Delivery Rev.* **2004**, *56*, 95–115.

[4] E. W. Kellogg III, I. Fridovich, *J. Biol. Chem.* **1975**, *250*, 8812–8817.

[5] M. Ochs, S. Carregal-Romero, J. Rejman, K. Braeckmans, S. C. De Smedt, W. J. Parak, *Angew. Chem. Int. Ed.* **2013**, *52*, 695–699; *Angew. Chem.* **2013**, *125*, 723–727.

[6] A. Fraix, A. R. Gonçalves, V. Cardile, A. C. E. Graziano, T. A. Theodossiou, K. Yannakopoulou, S. Sortino, *Chem. Asian J.* **2013**, *8*, 2634–2641.

[7] a) B. Fisher, J. P. Costantino, D. L. Wickerham, C. K. Redmond, M. Kavanah, W. M. Cronin, V. Vogel, A. Robidoux, N. Dimitrov, J. Atkins, M. Daly, S. Wieand, E. Tan-Chiu, L. Ford, N. Wolmark, *J. Natl. Cancer Inst.* **1998**, *90*, 1371–1388; b) C. K. Osborne, *N. Engl. J. Med.* **1998**, *339*, 1609–1618.

[8] M. M. Buckley, K. L. Goa, *Drugs* **1989**, *37*, 451–490.

[9] P. Diel, K. Smolnikar, H. Michna, *Breast Cancer Res. Treat.* **1999**, *58*, 87–97.

[10] a) M. Kandouz, A. Lombet, J. Y. Perrot, D. Jacob, S. Carvajal, A. Kazem, W. Rostene, A. Therwath, A. Gompel, *J. Steroid Biochem. Mol. Biol.* **1999**, *69*, 463–471; b) S. Salami, F. Karami-Tehrani, *Clin. Biochem.* **2003**, *36*, 247–253; c) S. Somai, M. Chaouat, D. Jacob, J. Y. Perrot, W. Rostene, P. Forgez, A. Gompel, *Int. J. Cancer* **2003**, *105*, 607–612.

[11] T. A. Theodossiou, K. Yannakopoulou, C. Aggelidou, J. S. Hothersall, *Photochem. Photobiol.* **2012**, *88*, 1016–1022.

[12] a) J. S. Manka, D. S. Lawrence, *Tetrahedron Lett.* **1989**, *30*, 7341–8022; b) J. S. Manka, D. S. Lawrence, *J. Am. Chem. Soc.* **1990**, *112*, 2440–2442; c) D. L. Dick, T. V. S. Rao, D. Sukumaran, D. S. Lawrence, *J. Am. Chem. Soc.* **1992**, *114*, 2664–2669; d) T. Carofiglio, R. Fomasier, V. Lucchinic, C. Rosso, U. Tonellato, *Tetrahedron Lett.* **1996**, *37*, 8019–8022; e) D. Demore, A. Kasselouri, O. Bourdon, J. Blais, G. Mahuzier, P. Prognon, *Appl. Spectrosc.* **1999**, *53*, 180A–194A; f) K. Kano, R. Nishiyabu, T. Asada, Y. Kuroda, *J. Am. Chem. Soc.* **2002**, *124*, 9937–9944; g) K. Kano, R. Nishiyabu, R. Doi, *J. Org. Chem.* **2005**, *70*, 3667–3673.

[13] a) J. Moan, K. Berg, H. Anholt, K. Madslien, *Int. J. Cancer* **1994**, *58*, 865–870; b) K. Berg, K. Madslien, J. C. Bommer, R. Oftebro, J. W. Winkelman, J. Moan, *Photochem. Photobiol.* **1991**, *53*, 203–210.

[14] D. V. Sakharov, E. D. Elstak, B. Chernyak, K. W. Wirtz, *FEBS Lett.* **2005**, *579*, 1255–1260.

[15] a) O. J. Norum, P. K. Selbo, A. Weyergang, K. E. Giercksky, K. Berg, *J. Photochem. Photobiol.* **2009**, *96*, 83–92; b) K. Berg, M. Berstad, L. Prasmickaite, A. Weyergang, P. K. Selbo, I. Hedfors, A. Hogset, *Top. Curr. Chem.* **2010**, *296*, 251–281; c) K. Berg, P. K. Selbo, L. Prasmickaite, A. Hogset, *Curr. Opin. Mol. Ther.* **2004**, *6*, 279–287.

Received: January 8, 2015
Published online: February 6, 2015

